

To cite this article: HUANG Y C, HE Y P, QIU M, et al. Overall vibration-reduction technology of FPSO topsides based on elastic connection [J/OL]. Chinese Journal of Ship Research, 2024, 19(3). <http://www.ship-research.com/en/article/doi/10.19693/j.issn.1673-3185.03304> (in both Chinese and English).

DOI: 10.19693/j.issn.1673-3185.03304

Overall vibration–reduction technology of FPSO topsides based on elastic connection



HUANG Yucu^{1,2,3}, HE Yanping^{*1,2,3}, QIU Ming⁴, LIU Yadong^{1,2,3}, LI Mingzhi^{1,2,3}

1 State Key Laboratory of Ocean Engineering, Shanghai Jiao Tong University, Shanghai 200240, China

2 School of Ocean and Civil Engineering, Shanghai Jiao Tong University, Shanghai 200240, China

3 Institute of Marine Equipment, Shanghai Jiao Tong University, Shanghai 200240, China

4 COSCO Shipping (Qidong) Offshore Co., Ltd., Qidong 226259, China

Abstract: [Objective] In order to decrease the vibration response of topside modules and reduce the transmission of vibration energy from topsides to hull, as well as improving the connection between topsides and hull, this paper proposes an overall vibration-reduction technology that is with the topsides connecting elastically to the hull of a floating production storage and offloading (FPSO) unit. [Methods] In this vibration-reduction technology, elastomeric bearing pads are utilized to connect the topsides to the hull, and the design loads and inner structure of the pads are determined by predicting the maximum values of the FPSO's acceleration response. The force and corresponding deformation of a specific elastomeric bearing pad are analyzed by the finite element method, and the equivalent stiffness of this pad is obtained as the slope of linear fitting. The vibration response of the topsides and power transmission characteristics of the elastomeric supporting system are then analyzed via numerical simulation and theoretical analysis respectively, with the elastomeric bearing pads replaced with linear springs correspondingly. [Results] The vibration responses of the topsides are effectively reduced, with the vibration reduction ratio as high as 30%, while the vibration isolation of the hull can also be effective with the appropriate selection of frequency ratio. [Conclusion] This study can provide valuable references for the design and application of the overall vibration reduction of topsides on offshore structures.

Key words: floating production storage and offloading (FPSO); topside module; elastic connection; overall vibration-reduction

CLC number: U661.44

0 Introduction

Floating production storage and offloading (FPSO) is one of the main equipment for the development of offshore oil and gas resources, and the various functional modules on the upper part of its main deck play an important role in the commercial exploitation of oil and gas resources. The topside modules are supported on the main deck by specific structures so as to be connected to the hull. The supporting structures usually include various types such as columns, crossbeams and stools^[1-3], as shown in Fig. 1. The shapes and sizes of supporting structures in the same type may vary depending on the weight of topsides or the sea state of the operating area. Column supporting is a way

that usually supports topsides through columns at multiple points on the strong ribs, transverse bulkheads or longitudinal bulkheads of the deck. Crossbeam supporting is the use of a certain height of the crossbeam structure to support topsides. Its position is often aligned with the strong ribs of hull, the length is generally uninterrupted from port to starboard, and the number depends on the longitudinal span of topsides. Stool supporting is a widely used support method in recent years. Usually, topsides are supported on several stools, which are positioned at the deck strengthening position. For the lighter topside modules, the stools are generally smaller and the structure is relatively simple; while for the heavier topside modules, the stool structure is more complex, with thicker plates

and larger sizes [4-6].

If the sea conditions are good, such as the Bohai Sea, topsides and the hull are usually rigidly connected by the supporting structure. Thus topsides and the hull are connected as one, which is more solid and safer. However, when FPSO is located in the poor sea conditions such as the South China Sea, it may cause a large wave bending moment on the hull. It will not only intensify the force and deformation of topsides, but also easily cause fatigue crack and even fractures in the welds between the supporting structure and the deck. Therefore, when operating in poor sea conditions, FPSO should not use rigid way to connect topsides with the hull. Instead, a mixture of fixed stools and sliding stools should be used to connect them, so that the relative sliding between stools and modules can release the stress caused by the overall longitudinal bending of the hull on topsides, thereby reducing the adverse effects of the hull

deformation on topsides. However, this connection will result in a large stress concentration near the connection between the fixed stools and topsides, and the relative sliding between topsides and the stools will generate a large noise. To maximize the stress relief of topsides, the ideal way is to divide topsides and the hull into two parts, so all the sliding stools can also be used for the connection. However, when the ship undergoes a more intense heave motion, the risk of topsides detaching from the deck stools is higher, so this connection is applicable to smooth sea areas [7-15].

Liu [16], Du [17], Shang et al. [18], Liu et al. [19] and Liu et al. [20] considered that spherical bearing pads can be installed between topsides and deck stools, where the top and bottom of the spherical bearing pads are welded to the bottom of the module legs and the top of the deck stools, respectively. This utilizes the relative rotation or sliding performance of the spherical bearing structure to release the large concentrated stress near the module legs. In addition, the horizontal movement of topsides can be elastically limited by the limiting structure with elastomeric bearing pads, while also limiting the uplift motion of the module. This connection effectively relieves the severe stress concentration phenomenon caused by the overall longitudinal bending of hull at the connection between topsides and the deck stools, which has been successfully applied in actual projects. However, the existing spherical bearing pads do not yet have vibration-reduction function for high-frequency vibrations caused by the internal excitation sources of topsides.

Xu [21-23] introduced an elastic connection method with vibration-reduction function, in which spherical bearing pads are replaced by elastomeric bearing pads, and a limiting structure with elastomeric bearing pads is also configured horizontally to limit the horizontal movement of the module. This method utilizes the elastomeric bearing pads with strong bearing capacity and high stiffness to elastically support topsides, thus realizing the vibration-reduction effect of the support system on topsides. Due to the use of horizontal elastic limit, when the hull undergoes overall longitudinal bending, the compression deformation of vertical elastomeric bearing pads can buffer a certain amount of hull bending, thus reducing the additional force and deformation of topsides caused by hull deformation. Considering the safety of topsides, the connection adopts a rigid



(a) Column supporting^[11]



(b) Crossbeam supporting^[12]



(c) Stool supporting^[13]

Fig. 1 The supporting styles of topsides on FPSO

anti-uplift claw to limit the uplift motion of topsides, but the rigid anti-uplift claw will weaken the buffer capacity of elastomeric bearing pads for hull deformation.

The target ship FPSO studied in this paper is proposed to adopt the elastic connection between topsides and hull, that is, the elastomeric bearing pads are used to limit, support and anti-uplift topsides in both horizontal and vertical directions, as shown in Fig. 2. Compared with the elastic connection mentioned above, the target ship FPSO will use elastomeric bearing pads to anti-uplift the motion of topsides. In this way, while using the elastomeric bearing pads to reduce the overall vibration of topsides, the compression deformation of the elastomeric bearing pads can be utilized to buffer the overall longitudinal bending of hull to a greater extent, so as to minimize the adverse effects on topsides and give full play to the elasticity of elastomeric bearing pads. Therefore, this paper intends to study the overall vibration-reduction technology of FPSO topsides based on elastic connection. By determining the design load and internal structure of elastomeric bearing pads, the bearing capacity and equivalent stiffness of elastomeric bearing pads are calculated. Then the paper analyzes the vibration-reduction effect of topsides and the vibration isolation characteristics of the elastomeric supporting system to evaluate the application effect of this vibration-reduction technology.

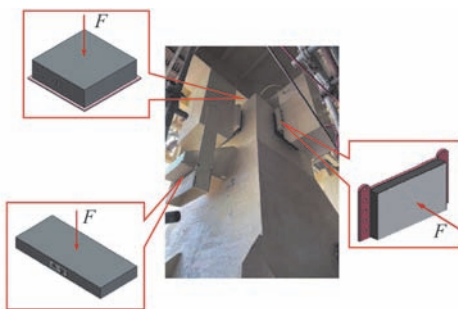


Fig. 2 Elastic connection between topsides and hull around a stool on FPSO

1 Overall vibration reduction design of topside modules

In this section, the overall vibration-reduction design of FPSO topsides will be introduced by taking a stool and its surrounding connection structure as examples. As shown in Fig. 3, the vertical elastomeric bearing pads are fixed on the top of the deck stool, and its top surface is in

connection with the bottom of the module leg, which mainly bears the vertical load from topsides. When the module carries out oil and gas treatment, the internal machinery equipment will generate high-frequency vibration, and the vibration energy will be partially absorbed and dissipated by the vertical elastomeric bearing pads in the process of transmitting to the hull, so as to isolate the part of vibration energy. The bottom structure of the module leg has two limit structures welded symmetrically in the horizontal and vertical directions, in which one end of the horizontal elastomeric bearing pads is fixed on the limit structure, and the other end is in connection with the deck stools, thus playing a buffering role in restricting the horizontal movement of topsides. To limit the uplift motion of the module, an anti-uplift structure is welded to each of the 2 longitudinal horizontal limit structures, which is in connection with the deck stools through the anti-uplift elastomeric bearing pads. It should be noted that the horizontal elastomeric bearing pads and the anti-uplift elastomeric bearing pads are only involved in the motion limit and buffering of topsides, but not in the overall vibration-reduction of topsides. When considering the impact of the reduced overall longitudinal bending of the hull on topsides, the gap between the vertical and anti-uplift elastomeric bearing pads and the deck stools can be adjusted as needed, or the installation of the vertical and anti-uplift elastomeric bearing pads can be canceled as appropriate.

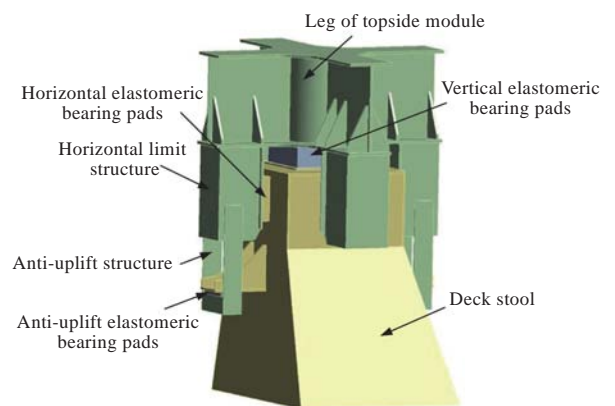


Fig. 3 Vibration-reduction design of topsides around a stool on FPSO

2 Bearing capacity and stiffness of elastomeric bearing pads

2.1 Design external load of elastomeric bearing pads

Oil and gas materials are transported through the

pipeline between topsides and pipe gallery, as well as between adjacent topsides. Therefore, the stiffness of elastomeric bearing pads should not be too small. Otherwise, excessive deformation of elastomeric bearing pads may cause significant relative displacement between modules and the pipe gallery or between the adjacent modules, resulting in significant shear force on the pipeline. In the long run, it is easy to lead to deformation or even fracture of the pipeline. At the same time, the stiffness of elastomeric bearing pads should not be too large, otherwise it is impossible to achieve overall vibration reduction and elastic limit of topsides.

Due to the large mass of topsides, often up to several thousand tons, normal elastic elements such as springs or rubber cannot withstand their weight. Laminated rubber bearing used in the field of civil engineering for the seismic resistance of large buildings or bridges on land has a strong load-bearing capacity, sufficient to carry the weight of large buildings or bridges without damage. It is possible to use its elasticity and damping characteristics to absorb and dissipate the energy of seismic waves, thus achieving the effect of seismic resistance. Therefore, reference can be made to the land-based seismic design of laminated rubber bearings, which can be applied to the vibration reduction of marine structures on topsides and the vibration isolation of ship hulls. In this paper, laminated rubber bearings are applied to FPSO as elastomeric bearing pads to support the weight of topsides and reduce vibration of topsides and isolate vibration of hull during oil and gas processing.

Laminated rubber bearing consists of rubber and thin steel plate, which are chemically cemented as a whole. Its cross-section is shown in Fig. 4. The number and thickness of the thin steel plates inside the elastomeric bearing pads can be adjusted as needed to change its bearing capacity and stiffness, but the thickness and other parameters should meet the requirements of standardization [24].

Fig. 5 shows the arrangement of topsides on the main deck of FPSO. The parameters of topside module MW01 are shown in Table 1. 1) The center of gravity position 1 is the center of gravity position of the module relative to its own coordinate system, that is, the midpoint of the intersection line of the module base plane and the plane near the stern is taken as the coordinate origin. The direction from

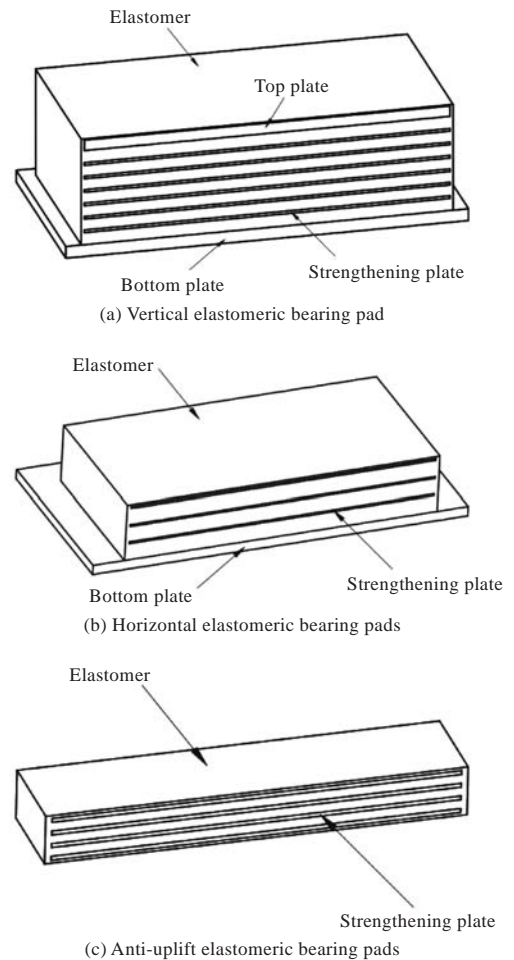


Fig. 4 Diagrams of the elastomeric bearing pads in cross section

the origin to the bow is the positive X -axis direction, the direction to the port is the positive Y -axis direction, and the vertical upward is the positive Z -axis direction. 2) The center of gravity position 2 is the center of gravity position of topsides relative to the hull coordinate system.

Among the numerous topside modules, MW01 has the largest weight and its center of gravity is the furthest from the ship, so MW01 receives the largest inertia force when the ship is moving. Therefore, the module MW01 is used as a representative to determine the design load of elastomeric bearing pads. The force and deformation of elastomeric bearing pads are closely related to the ship motion response, which is affected by the environmental conditions. The design load of elastomeric bearing pads can be calculated according to the extreme value of ship acceleration response under extreme sea conditions. The extreme sea conditions in the operation area, the mooring arrangement scheme of FPSO, the corresponding numerical model, and prediction results and research findings of related motion

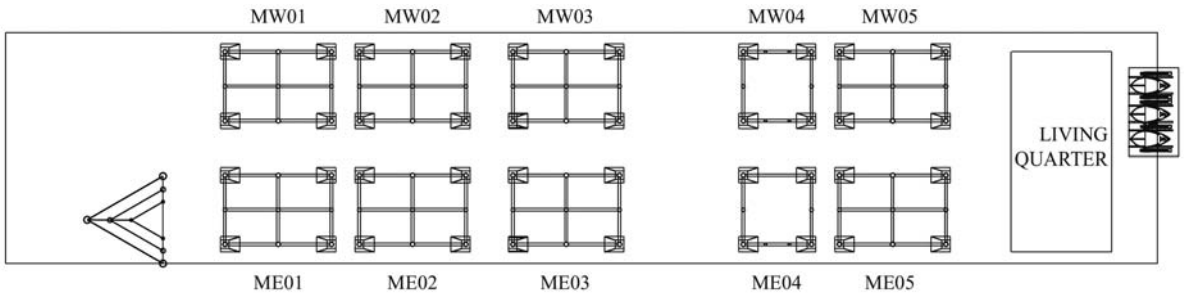


Fig. 5 Arrangement of topsides on the main deck of FPSO

responses are shown in Reference [25], which will not be repeated here for the length limitation.

According to the prediction results of ship acceleration response, when FPSO is in the ballast state under extreme sea conditions, the vertical motion acceleration caused by the ship pitch motion at the position of the topside module MW01 is the highest (0.58 m/s^2). However, the topside modules and the deck stools are two separate parts. Considering the relative motion of topsides and the hull, the dynamic force of topside module MW01 on the vertical elastomeric bearing pads must be larger than the force generated by the acceleration of 0.58 m/s^2 . Referring to the "Code for anti-collapse design of building structures"^[26] and code for marine engineering design DNVGL-OS-C101^[27], the dynamic coefficient is taken as 2.0, namely, when considering the interaction between topsides and the hull, the design load of vertical elastomeric bearing pads is taken to be 2 times of the static load of topsides. Assuming that the weight of topsides is uniformly distributed to the four deck stools, the design load of a vertical elastomeric bearing pad is 19.30 MN. The anti-uplift elastomeric bearing pads are usually in an unstressed state. Only when the ship moves upward to reach the highest point, there is a short relative motion between the hull and topsides because of inertia. At this time, the hull is moving downward, while topsides are still upward. The hull squeezes the anti-uplift elastomeric bearing pads to drive topsides downward, which causes the anti-uplift elastomeric bearing pads to be in the loading state. It can be considered that hull is the object applying

the force and topsides are the objects bearing the force. The maximum vertical acceleration response 0.58 m/s^2 of FPSO at module MW01 is taken as a reference. It is assumed that the hull uniformly exerts force on topside modules through the anti-uplift elastomeric bearing pads. The safety factor is taken as 2.0. Then the design load of an anti-uplift elastomeric bearing pad can be calculated as 4.64 MN based on the number of topside modules and anti-uplift elastomeric bearing pads. Under extreme sea conditions, When FPSO is in a ballast state, the horizontal acceleration caused by the ship surge motion at the topside module MW01 is the largest (0.32 m/s^2). Taking this acceleration response value as a reference, the safety factor is taken as 2.0. Assuming that the horizontal elastomeric bearing pads on the four stools are uniformly stressed when topsides and the hull undergo horizontal relative motion, the design load of a horizontal elastomeric bearing pad can be calculated as 0.63 MN.

2.2 Stiffness of elastomeric bearing pads

The parameters and sizes of elastomeric bearing pads are shown in Table 2 and Table 3, respectively. In this paper, the two-parameter Mooney-Rivlin hyperelastic constitutive model will be used to simulate the rubber material, and numerical models of vertical elastomeric bearing pads, horizontal elastomeric bearing pads and anti-uplift elastomeric bearing pads will be established. The finite element method will be used for the external load and stress distribution of elastomeric bearing pads under a certain deformation amount, so as to determine the bearing capacity of elastomeric bearing pads. In Table 2, C_{10} and C_1 are the two parameters in the two-parameter Mooney-Rivlin hyperelastic constitutive model. According to the arrangement of elastomeric bearing pads, when topsides and the hull are in relative motion, each elastomeric bearing pad mainly bears vertical pressure, so the vertical force and deformation characteristics of elastomeric

Table 1 Parameters of topside module MW01

Parameters	Values
Mass/t	3 934
Size/m	31.8×20.2×19.5
Center of gravity position 1/m	(15.9, 0, 15.1)
Center of gravity position 2/m	(63.9, 14.4, 50.5)

bearing pads should be analyzed.

Table 2 Parameters of elastomeric bearing pads

Materials	Parameters	Values
Rubber	Density/($\text{kg}\cdot\text{m}^{-3}$)	1 000
	M-R model	$C_{10}=0.474$
		$C_1=0.118$
	Poisson's ratio	0.49
	Yield strength/MPa	15
Steel plate	Density/($\text{kg}\cdot\text{m}^{-3}$)	7 850
	Young's modulus/GPa	200
	Poisson's ratio	0.29
	Yield strength/MPa	355

Table 3 The sizes of elastomeric bearing pads

Name	Overall sizes/mm		
	Vertical elastomeric bearing pads	Anti-uptilt elastomeric bearing pads	Horizontal elastomeric bearing pads
Overall	1 300×1 300×400	650×300×75	960×960×175
Bottom plate	1 300×1 300×40		960×960×25
Elastomer	1 200×1 200×360	650×300×75	800×800×150
Top plate	1 180×1 180×35.5		
Strengthening plate	1 180×1 180×9.0	630×280×6.5	780×780×5.0

The finite element analysis process of the elastomeric bearing pads is shown in Fig. 6. Firstly, a three-dimensional model is established according to the material parameters and sizes of elastomeric bearing pads. Then the three-dimensional model is meshed to obtain a finite element model. Based on this, boundary conditions are set for finite element analysis of each elastomeric bearing pad. The two boundary conditions for finite element analysis are: 1) fixed constraints are imposed on the bottom of the elastomeric bearing pads to simulate its fixation on the corresponding structure; 2) vertical compression deformation is applied to the top surface of the elastomeric bearing pads to simulate the deformation caused by the vertical pressure when topsides are moving relative to the deck stools and the initial value of the deformation is 1 mm. Referring to the load and resistance factor design (LRFD) method in code for marine engineering design DNVGL-OS-C101^[27], the safety factor of the material is taken as 1.15. Then the safety factor of the steel plate and rubber can be calculated by combining with the yield strength of the material. If the safety factor is greater than 1.15, the vertical compression in the boundary conditions can be increased by 1 mm on the basis of the

original value. Other settings remain unchanged to continue the finite element analysis of the elastomeric bearing pads. When the safety factor of the steel plate or rubber is less than or equal to 1.15, the finite element analysis can be stopped. After the finite element analysis, the vertical pressure of each elastomeric bearing pad in a specific compression deformation and the maximum stress of steel plate and rubber can be obtained.

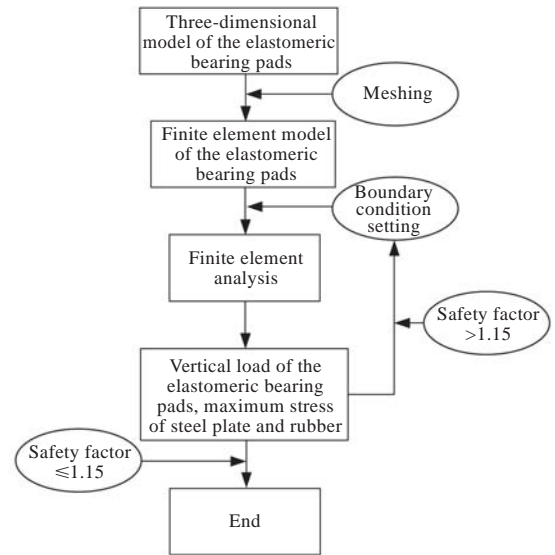


Fig. 6 Finite element analysis process of the elastomeric bearing pads

2.2.1 Verification of finite element method

Before the finite element analysis, the finite element method was verified to ensure the accuracy of the calculation in this paper. The finite element method was used to repeat the shear experiment conducted by Han et al. ^[28-29] on the elastomeric bearing pads, so as to compare the finite element analysis results with the experimental results to verify the accuracy of the method. The parameters, sizes, and experimental operations of the elastomeric bearing pads are described in detail in the original paper, so they will not be repeated in this paper due to space limitation. In the verification process, a hexahedral mesh was used as the main meshing method for the elastomeric bearing pads, and the finite element model is shown in Fig. 7. Fixed constraints were applied to the bottom of the model, and the horizontal tangential deformation was imposed on the elastomeric bearing pads. The initial value of tangential deformation was 10 mm, followed by an increase of 10 mm in deformation. A total of 10 finite element analyses were carried out, and the tangential deformation increased from 10 mm to 100 mm.

Comparisons of the results between finite element analysis and experiment in horizontal shear force are shown in Fig. 8. As can be seen, although there are some errors in the finite element analysis results of shear force, in general, they are in good agreement with the experimental results, which verifies the accuracy and feasibility of using the finite element method to analyze the force of elastomeric bearing pads.

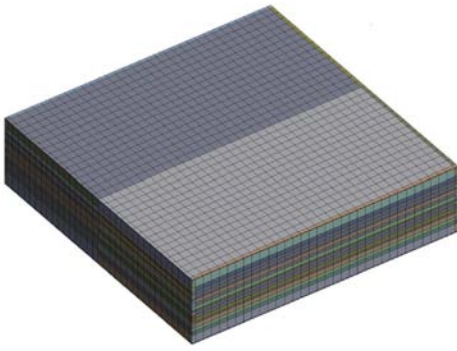


Fig. 7 Finite element model of elastomeric bearing pad for verification

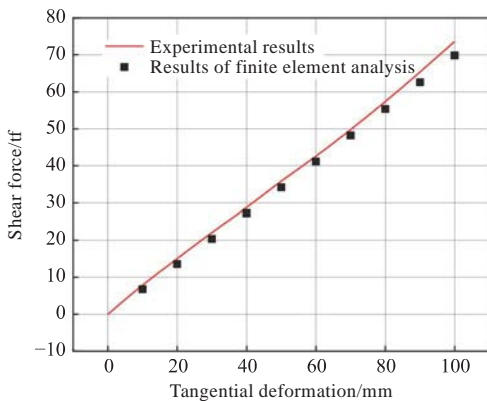


Fig. 8 Comparisons of the results between finite element analysis and experiment^[28-29]

2.2.2 Mesh independent analysis

This paper mainly adopts the hexahedral mesh to mesh the vertical, horizontal and anti-uplift elastomeric bearing pads. Since the mesh mass will directly affect the calculation accuracy of the finite element method, it is necessary to conduct mesh independent analysis on three types of elastomeric bearing pads based on four mesh parameters: mesh number, node number, average mass of mesh, and twist degree. The operating modes of vertical and horizontal elastomeric bearing pads will be analyzed with 10 mm compression deformation, and the operating mode of the anti-uplift elastomeric bearing pads will be analyzed with 4 mm compression deformation. The results of the mesh independent analysis are shown in Table 4–Table 6.

mesh independent analysis, the calculated vertical pressures of the vertical, horizontal and anti-uplift elastomeric bearing pads with three mesh sizes are relatively close or even the same, which indicates that the calculation results are independent of the selected mesh sizes. However, changes in mesh sizes will cause variations in the number of meshes and nodes, which results in the difference in calculation efficiency. For the three selected mesh sizes, the difference in the numerical calculation time for the horizontal and anti-uplift elastomeric bearing pads is relatively small, but the numerical calculation time for the vertical elastomeric bearing pads is more sensitive to mesh sizes. The numerical calculation time corresponding to the mesh sizes of 30, 15, 10 mm is about 0.5, 1, 4 h, respectively. Therefore, in order to balance the accuracy and efficiency of numerical calculation, the mesh sizes of 30, 10, 10 mm are used for the vertical, horizontal, and anti-uplift elastomeric bearing pads respectively in the subsequent finite element analysis.

Table 4 Mesh independent analysis results of the vertical elastomeric bearing pads

Mesh sizes/mm	Mesh number	Node number	Average mass	Average twist degree	Vertical pressure/MN
30	72017	77612	0.55	6.4×10^{-2}	31.2
15	271373	285755	0.88	2.6×10^{-2}	30.9
10	673144	701036	0.97	1.8×10^{-3}	30.0

Table 5 Mesh independent analysis results of the horizontal elastomeric bearing pads

Mesh sizes/mm	Mesh number	Node number	Average mass	Average twist degree	Vertical pressure/MN
40	11312	12977	0.34	8.4×10^{-2}	10.6
20	40141	44500	0.64	3.3×10^{-2}	10.4
10	149248	162295	0.92	8.0×10^{-4}	10.4

Table 6 Mesh independent analysis results of the anti-uplift elastomeric bearing pads

Mesh sizes/mm	Mesh number	Node number	Average mass	Average twist degree	Vertical pressure/MN
30	3312	4056	0.39	3.7×10^{-2}	6.1
20	6528	7735	0.57	3.1×10^{-2}	6.1
10	23400	26598	0.90	8.5×10^{-3}	6.1

2.2.3 Equivalent stiffness of elastomeric bearing pads

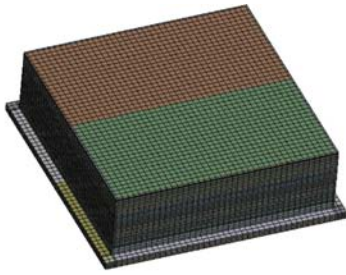
The meshing results of three-type elastomeric bearing pads are shown in Fig. 9, and their finite element analysis results and safety factors are shown in Table 7 to Table 9. Fig. 10 shows the

From Table 4 to Table 6, it can be seen that in the

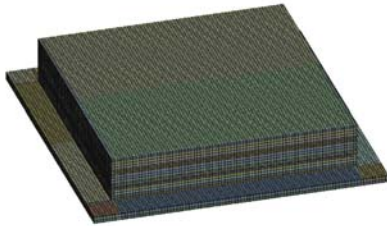
finite element analysis results of the vertical, horizontal and anti-uplift elastomeric bearing pads with vertical compression deformations of 10, 10,

4 mm, respectively.

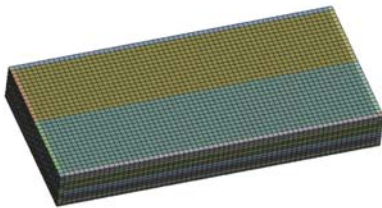
Since the vertical compression deformation of the elastomeric bearing pads is relatively small, it can be assumed that there is a linear relationship between the external force and deformation. Using the least square method, *xy* linear fitting was performed on the corresponding data points of the vertical external force and compression deformation of the elastomeric bearing pads in Table 7 to



(a) Vertical elastomeric bearing pads



(b) Horizontal elastomeric bearing pads

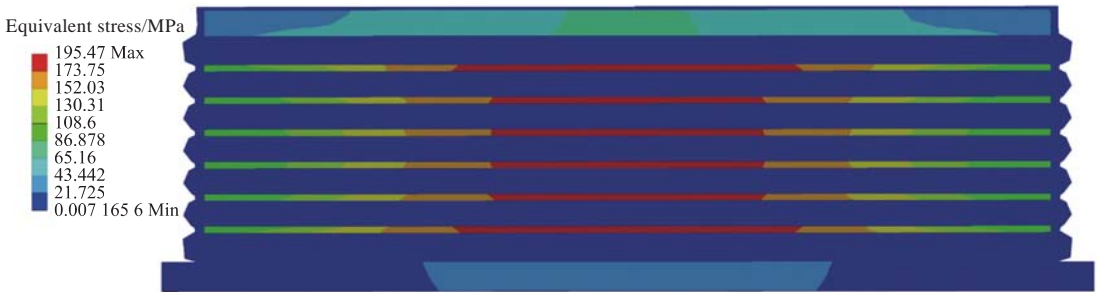


(c) Anti-uplift elastomeric bearing pads

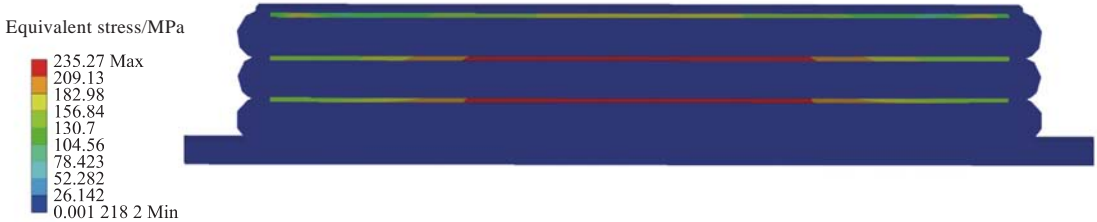
Fig. 9 Meshing of the elastomeric bearing pads

Table 7 Finite element analysis results of vertical elastomeric bearing pads

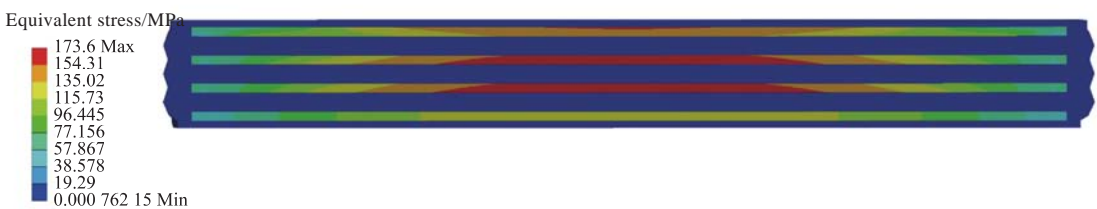
Compression deformation /mm	Vertical external force/MN	Maximum stress of steel plate/MPa	Safety factor	Maximum stress of rubber/MPa	Safety factor
0	0	0		0	
1	2.8	18.7	19.0	0.4	37.5
2	5.7	37.7	9.4	0.9	16.7
3	8.7	56.8	6.3	1.3	11.5
4	11.7	76.1	4.7	1.9	7.9
5	14.8	95.6	3.7	2.4	6.3
6	17.9	115.3	3.1	3.1	4.8
7	21.2	135.0	2.6	3.9	3.8
8	24.5	154.9	2.3	4.8	3.1
9	27.8	175.1	2.0	5.8	2.6
10	31.2	195.5	1.8	6.9	2.2



(a) Vertical elastomeric bearing pads



(b) Horizontal elastomeric bearing pads



(c) Anti-uplift elastomeric bearing pads

Fig. 10 Finite element analysis results of the elastomeric bearing pads

Table 9. The slope obtained is the equivalent stiffness of the corresponding pad. As shown in Fig. 11, the equivalent stiffness of a single vertical, horizontal, and anti-uplift elastomeric bearing pad is 3.0, 1.0, 1.5 MN/mm, respectively.

Table 8 Results of finite element analysis of horizontal elastomeric bearing pads

Compression deformation/mm	Vertical external force/MN	Maximum stress of steel plate/MPa	Safety factor	Maximum stress of rubber/MPa	Safety factor
0	0	0		0	
1	0.9	22.9	15.5	0.5	30
2	1.8	46.1	7.7	1.1	13.6
3	2.7	69.7	5.1	1.7	8.8
4	3.7	93.6	3.8	2.5	6.0
5	4.7	118.0	3.0	3.3	4.5
6	5.8	142.7	2.5	4.3	3.5
7	6.9	167.7	2.1	5.5	2.7
8	8.0	193.1	1.8	6.9	2.2
9	9.1	218.8	1.6	8.5	1.8
10	10.4	235.3	1.5	10.3	1.5

Table 9 Finite element analysis results of anti-uplift elastomeric bearing pads

Compression deformation/mm	Vertical external force/MN	Maximum stress of steel plate/MPa	Safety factor	Maximum stress of rubber/MPa	Safety factor
0	0	0		0	
1	1.2	37.4	9.5	1.0	15
2	2.6	78.7	4.5	2.6	5.8
3	4.3	124.1	2.9	5.5	2.7
4	6.1	173.6	2.0	10.2	1.5

3 Characteristic analysis of the overall vibration reduction on topside modules

The internal high-frequency vibration energy of topsides can be transmitted to the hull along the deck stools through the vertical elastomeric bearing pads, which can cause fatigue damage to the stool structure or hull structure in severe cases. At the same time, topside module is a multi-layer steel frame device with certain structural stiffness. Its internal vibration can cause its own structural vibration response, which will deteriorate the working environment and affect the physical health of the operators. Therefore, the application effect of the overall vibration reduction technology for the topsides should be evaluated from the vibration response of the module structure and the vibration

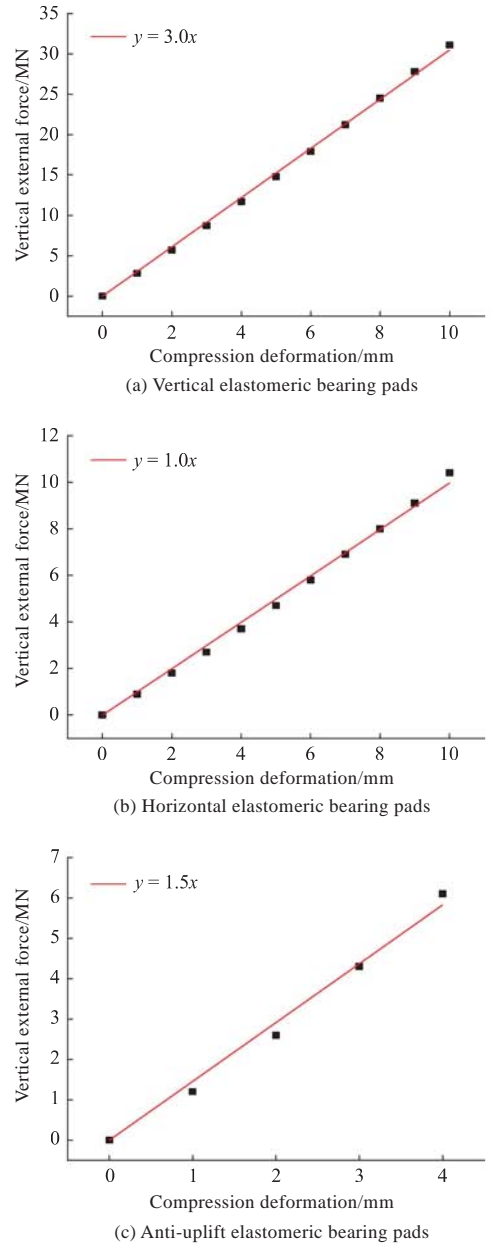


Fig. 11 Equivalent stiffness of elastomeric bearing pads

isolation performance of the elastomeric supporting system.

3.1 Vibration response of module structure

The three-dimensional model of topside module MW01 is established according to the drawings and documents. During the modeling process, the module structure can be simplified. For example, the structures of ladder, handrail and balustrade which do not affect the analysis results can be ignored. On the basis of the multi-layer frame structure of the module, according to the overall center of gravity position of the module, the mass distribution of the three-dimensional model can be adjusted by adding mass blocks. Hence, the total

mass and the center of gravity position of the three-dimensional model can be consistent with the actual values [30-31].

The main excitation sources in the module are two high-power pump devices located in the first deck, whose positions are shown in Fig. 12. The frequency range of the pumps during normal operation is 0.5–28 Hz, and the parameters of the excitation force are shown in Table 10. It is assumed that the excitation source has a regular shape, uniform mass, and its center of gravity is located at the geometric center. The unit excitation force or moment is applied at the center of gravity of the excitation source along the X , Z , RX , RY , and RZ directions, as shown in Fig. 13. The four support points at the bottom of the module are fixed and constrained. Then the harmonic response analysis is performed on the overall topside module MW01. The frequency range extends outward by 20% based on the operating frequency range of the excitation source, and frequencies below 1 Hz are ignored. The frequency range of the harmonic response analysis is finally determined to be 1–34 Hz.

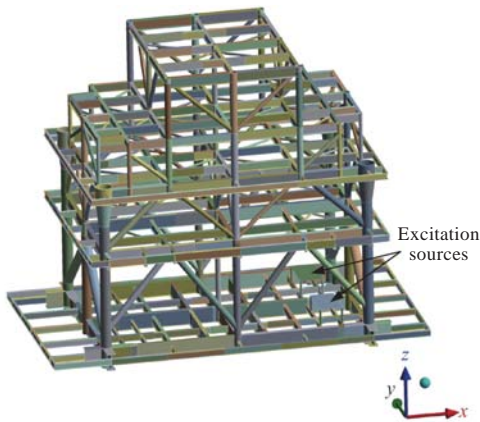


Fig. 12 Positions of excitation sources in the module

Table 10 Parameters of excitation force for an excitation source

Excitation force in different directions	Values
Excitation force in the X direction/N	884
Excitation force in the Z direction/N	884
Excitation force in the RX direction/(N·m)	416
Excitation force in the RY direction/(N·m)	49
Excitation force in the RZ direction/(N·m)	203

Referring to the relevant specification [32], the structural damping ratio of the multi-layer steel building is taken as 4%. The vibration responses of topside module MW01 in the X , Y , and Z directions under unit excitation force or moment in several directions are shown in Fig. 14. As can be seen, the

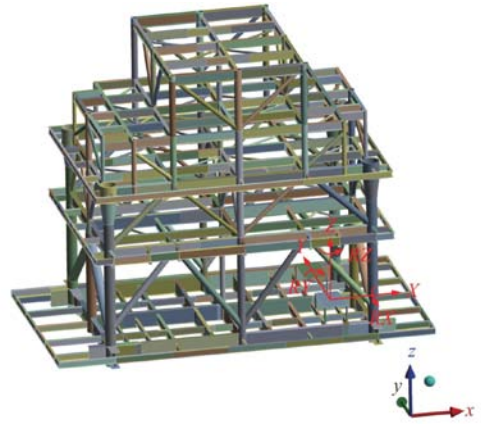


Fig. 13 Diagram of the excitation force for an excitation source

vibration response of the topside module structure is more significant when the excitation frequency is 4 Hz. Therefore,

working at a frequency of 4 Hz, the corresponding rated excitation force or moment is applied in the direction of each excitation force or moment simultaneously to simulate the vibration of topsides at work. Based on this, a comprehensive comparison of the vibration responses of topsides with and without overall vibration reduction is conducted to evaluate the vibration reduction effect.

When the vibration reduction of topside module is not considered, the 6 degrees of freedom at the bottom of the module legs are fixed as boundary conditions. When the overall vibration reduction of topside module is considered, the vertical elastomeric bearing pads are simulated by an equivalent spring, where the spring stiffness is equal to the equivalent stiffness of vertical elastomeric bearing pads and the damping ratio of elastomeric bearing pads is taken as 5% [33-34]. One end of the spring is connected to the bottom of module leg and the other end is connected to the ground.

When meshing the topside modules, the hexahedral mesh is dominated. Taking the topside module under elastic support as an example, mesh independent analysis is conducted, and the results are shown in Table 11.

It can be seen from Table 11 that the calculation results of the maximum acceleration vibration response of topsides are closer when the mesh sizes are 100 mm and 200 mm, while the calculation results have a larger error when the mesh size is 300 mm. It indicates that the calculation results tend to be stable when the mesh size is less than or equal to 200 mm. Therefore, in this paper, mesh

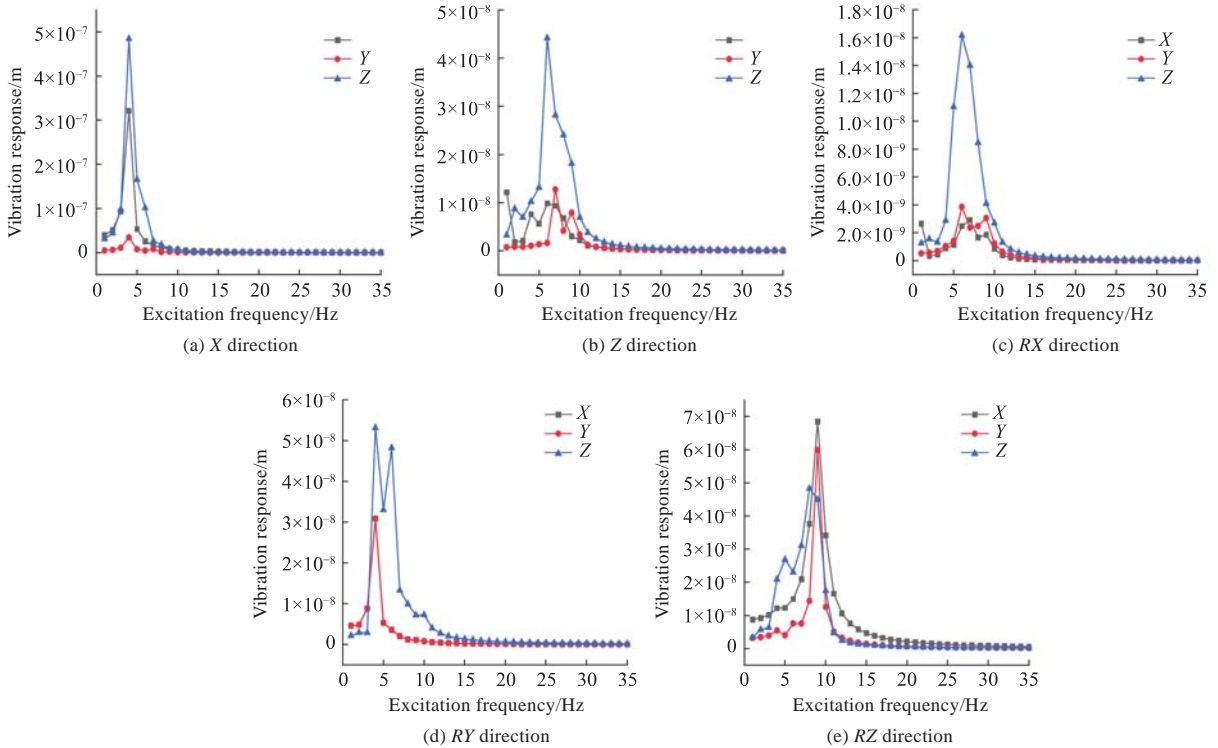


Fig. 14 Vibration responses of topside module MW01 under unit excitation force or moment in several directions

size of 100 mm was selected to mesh topsides, and the results are shown in Fig. 15.

Table 11 Mesh independent analysis results of the topside module

Mesh size /mm	Mesh number	Node number	Average mass	Average twist degree	Maximum acceleration $/(m \cdot s^{-2})$
300	478 721	459 671	0.80	0.160	0.253
200	549 163	541 428	0.84	0.100	0.187
100	1 035 287	1 029 864	0.90	0.059	0.184

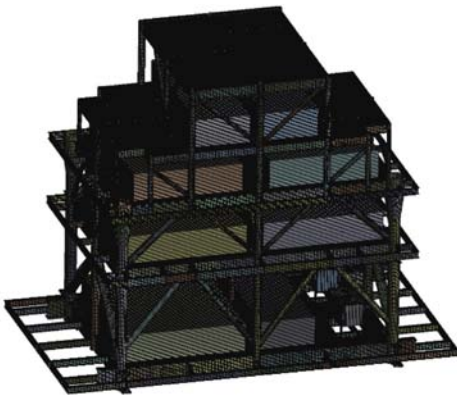


Fig. 15 Meshing of the topside module

The acceleration vibration responses of topsides with and without vibration reduction are shown in Fig. 16 and Fig. 17, respectively. The comparison results of the maximum acceleration response values in these two cases are shown in Table 12. BV specification [35] specifies the requirements for the working environment acceleration values of operators working on topsides. The acceleration

limits and requirements for operators working in all directions at a vibration frequency of 4 Hz are shown in Table 12.

When the overall topside module is damped, due to the elastomeric support at the bottom of the module, the top structure of the module will exhibit oscillatory responses under the internal excitation. The acceleration vibration response of the top structure will be increased at this time, but the response value is much smaller than the maximum acceleration vibration response of the module structure, as shown in Fig. 16(a). It indicates that the overall vibration reduction of topsides will not lead to a significant increase in the vibration response of the local module structure. As shown in Fig. 17(a), when the vibration reduction of topside module is not considered, the vibration response of the structure near the excitation sources and the same deck under the internal excitation is more significant. The weaker response occurs further away from the excitation source, which is mainly caused by the energy loss during vibration transmission due to the existence of structural damping. In addition, the energy loss will increase with distance.

From the comparison results of the maximum acceleration response values in Table 12, it can be seen that the maximum acceleration responses in the X, Y, Z directions of topsides with the overall

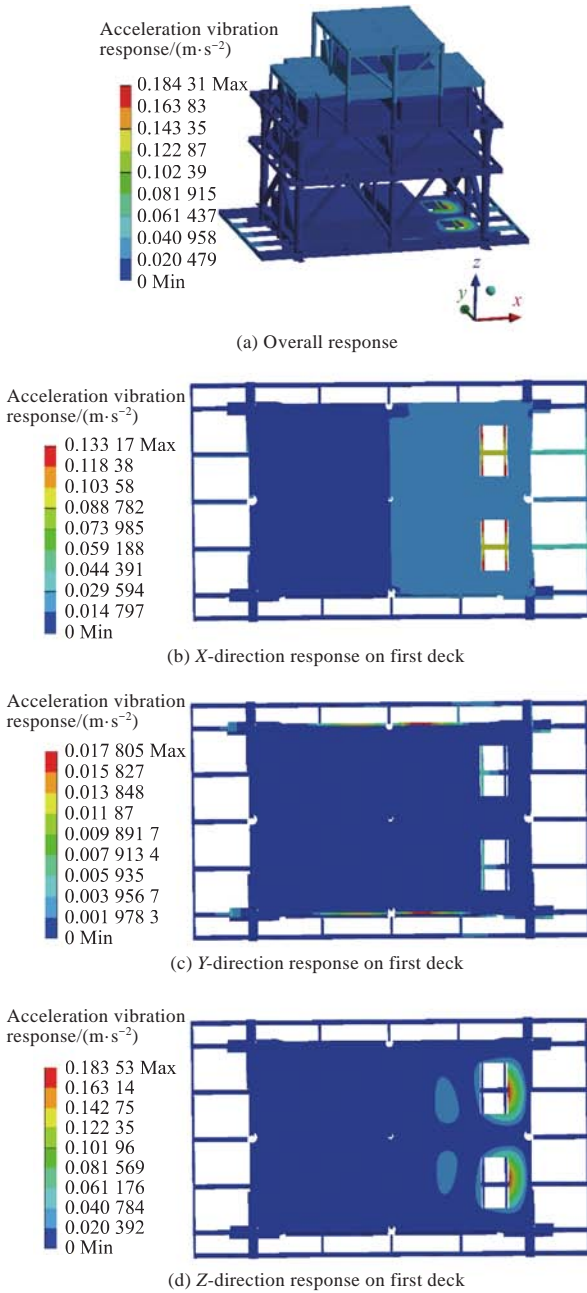


Fig. 16 Acceleration vibration responses of topside module with overall vibration-reduction

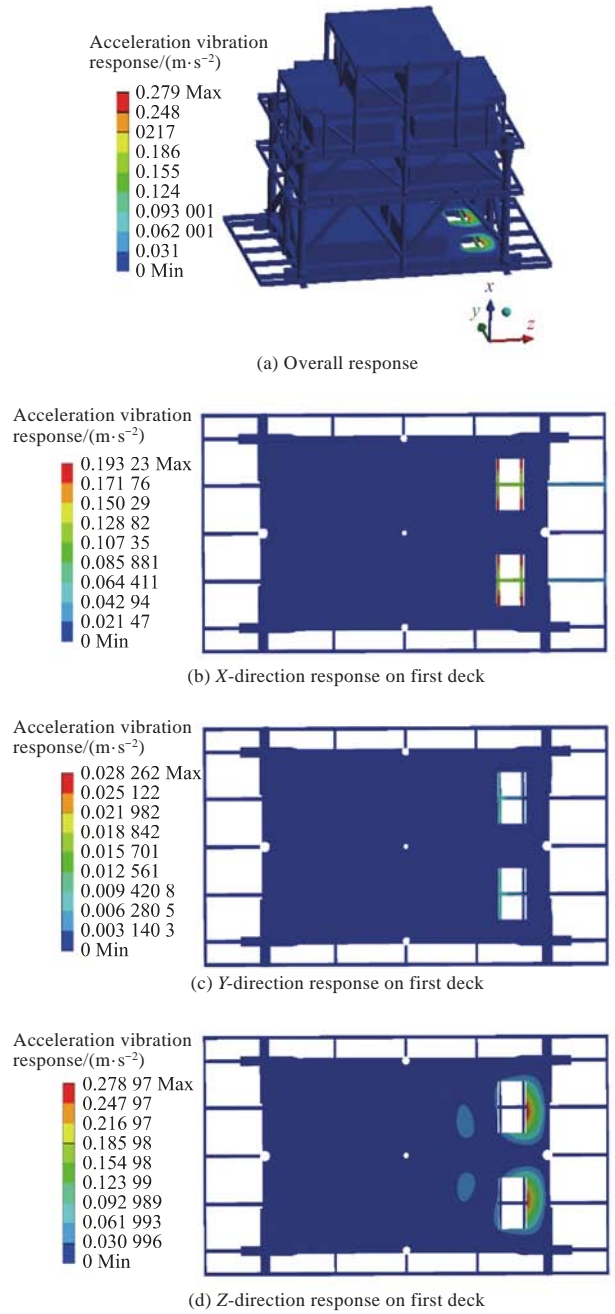


Fig. 17 Acceleration vibration responses of topside module without overall vibration-reduction

vibration reduction are less than the operating mode without vibration reduction, and the reduction efficiency is up to 30% or more. It indicates that the elastomeric supporting system of topsides does have the function of vibration reduction. The reasons are as follows: The topside module can be regarded as a steel frame with a certain structural stiffness, and it will exhibit vibration response under the high-frequency excitation of the internal excitation sources. When the overall vibration reduction is carried out at the bottom of the module, the vertical elastomeric bearing pads absorb and dissipate part of the vibration energy, which has a certain mitigation effect on the vibration of the

Table 12 Comparisons of maximum vibration response values of topside module with and without vibration-reduction

Response direction	Response with vibration reduction /($m \cdot s^{-2}$)	Response without vibration reduction /($m \cdot s^{-2}$)	Vibration reduction efficiency/%	Response value requirements of BV specification ^[35] /($m \cdot s^{-2}$)
X direction	0.133	0.193	31.1	≤ 0.3
Y direction	0.018	0.028	35.7	≤ 0.3
Z direction	0.184	0.279	34.1	≤ 0.26

module itself, so the vibration response of the module structure is weakened. According to Table 12, when the vibration reduction of topsides is not considered, the acceleration vibration response in the Z direction exceeds the maximum value

stipulated by the BV specification, which is not conducive to the health of the operators. When the overall vibration reduction of topsides is considered, the acceleration response in all directions of the module meets the requirements of the BV code. Therefore, adopting the overall vibration reduction technology for topsides will be beneficial in reducing the vibration response of the module structure, thus improving the working environment for operators.

The distribution of stress induced by excitation sources on first deck with and without vibration reduction of topsides is shown in Fig. 18, and the comparison of the maximum stress in these two cases is shown in Table 13.

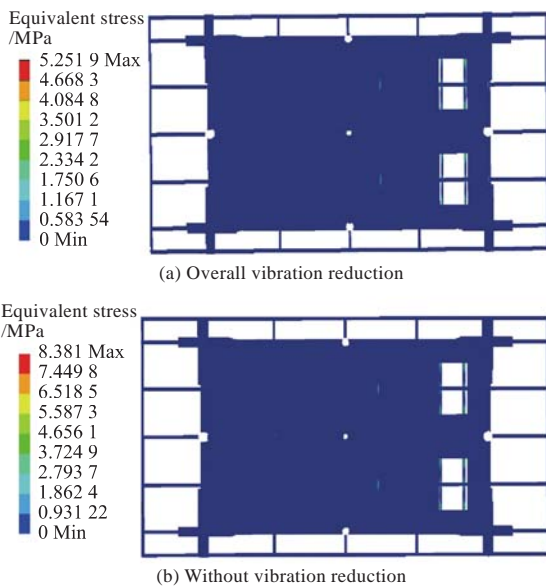


Fig. 18 Stress distribution on first deck induced by excitation sources with and without overall vibration-reduction

Consistent with the acceleration vibration response of topsides, Table 13 shows that the maximum stress of the module structure induced by excitation sources is reduced by 36.9% after the overall vibration reduction, and the reduction efficiency is also as high as 30% or more. As the finite element analysis in this paper only takes the two pumps in the topside module MW01 as an example, and the weight, volume and power of the pumps are relatively small, the structural stress caused by the vibration is also small. However, considering that the excitation sources in the module are generally more, the stress of the module structure may increase to a nonnegligible value under the superposition of vibration and gravity caused by multiple excitation sources. If the overall vibration reduction technology is adopted for topsides, the maximum value of the structural stress

can be significantly reduced, with a reduction efficiency of more than 30%. It is conducive to improving the fatigue life of topsides.

Table 13 Comparison of maximum stress induced by excitation sources on first deck with and without overall vibration-reduction

Name	Maximum stress with vibration reduction/MPa	Maximum stress without vibration reduction/MPa	Vibration reduction efficiency/%
Maximum stress with vibration reduction	5.3	8.4	36.9

3.2 Power transmission rate and vibration isolation efficiency of elastomeric supporting system

According to the vibration theory, the system comprised of the hull and a topside module can be regarded as a two-degree-of-freedom vibration system in the vertical direction, as shown in Fig. 19. The mass and the heave stiffness of the hull are M_1 and K_1 , respectively, and the mass of topside module and the equivalent rigidity of the vertical elastomeric bearing pads are M_2 and K_2 , respectively. Since the values of M_1 and K_1 are much larger than that of M_2 and K_2 , respectively, according to the two-degree-of-freedom vibration theory, the motions of M_1 and M_2 , namely, the motions of the hull and the topside module, almost do not affect each other and are independent of each other; Meanwhile, because the motion frequency of the FPSO hull is usually smaller than the vibration frequency of the ship machinery by one order of magnitude or more^[36], it can be considered that the hull is stationary. The vibration of the topside module can be detached from the overall motion of FPSO and studied separately. Hence, the two-degree-of-freedom vibration system can be simplified to a single-degree-of-freedom vibration system. Moreover, based on the regular shape of the topside module in the length and width, assuming that the internal mass of the module is uniformly distributed, and its center of gravity is located in the geometric center of the module horizontal plane, the weight of topsides is evenly distributed to the four elastomeric supporting points of the deck stools. Therefore, when studying the vibration of the topside module, the topside module supported by the four elastomeric supports can be further simplified, and finally only one of the elastomeric supports will be studied, that is, only the vibration isolation effect of the topside module elastically

supported on a deck stool will be studied.

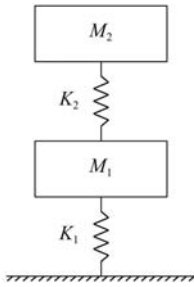


Fig. 19 Diagram of two-degree-of-freedom vibration system comprised of the hull and a topside module

In summary, the elastomeric supporting system consisting of the weight of topsides on a deck stool, a vertical elastomeric bearing pad and a deck stool is considered as a single-degree-of-freedom vibration isolation system in this paper. Here, only the vibration transmission in the vertical direction is considered. It is assumed that the topside module is an ideal rigid body, the vibration isolator (vertical elastomeric bearing pad) is composed of an ideal spring and an ideal damper without mass, and the base of the deck stools and the hull is a rigid body with an infinite mass, as shown in Fig. 20.

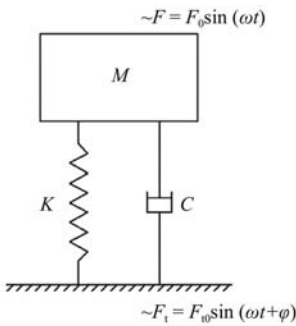


Fig. 20 Diagram of single-degree-of-freedom vibration-isolation system

In Fig. 20, F is the external excitation force of the vertical elastomeric bearing pads (varying sinusoidally), with the unit of N; F_0 is the amplitude of the excitation force; ω is the angular frequency of the excitation force, with the unit of rad/s; t is time in s; M is the mass of topsides corresponding to the gravitational load of a vertical elastomeric bearing pad, with the unit of kg; K is the elasticity coefficient of the equivalent spring, that is, the equivalent stiffness of the vertical elastomeric bearing pads, with the unit of N/m; C is the damping coefficient of the vertical elastomeric bearing pads, with the unit of N·s/m; F_t is the force transmitted to the base, called the transmitted force, with the unit of N; F_0 is the amplitude of the transmitted force; φ is the phase difference between the excitation force and the transmitted force in rad.

According to the single-degree-of-freedom vibration theory [36-37], the power transmission rate is a function of damping ratio and frequency ratio. The lower the power transmission rate, the higher the vibration isolation efficiency. With frequency ratio as the horizontal coordinate and power transmission rate as the vertical coordinate, the power transmission rate curves are drawn when damping ratios are 0, 0.05, 0.10, 0.20, 0.50, and 1.00 respectively, as shown in Fig. 21. All the power transmission rate curve intersects at the point $(\sqrt{2}, 1)$. When the frequency ratio is less than $\sqrt{2}$, the power transmission rate is greater than 1, indicating that the system does not have vibration isolation effect. Only when the frequency ratio is greater than $\sqrt{2}$, the power transmission rate is less than 1, indicating that the system has vibration isolation effect. The lower damping ratio will lead to more obvious vibration isolation effect. Thus, to achieve isolation effect for the high-frequency vibration energy transmitted from the topside module to the hull, the frequency ratio must be greater than $\sqrt{2}$. According to the computational formula of natural frequency $\omega_n = \sqrt{K/M}$, the natural frequency of single-degree-of-freedom isolation system is $\omega_n = 8.8$ Hz, which indicates that the elastomeric supporting system has a good isolation effect on excitation with frequency greater than 12.4 Hz. Therefore, it has a good isolation effect on most vibration devices of the module.

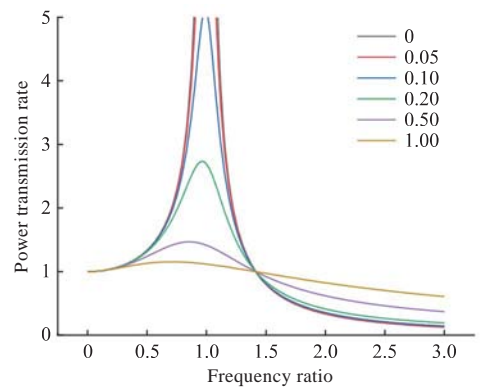


Fig. 21 Power transmission rates of single-degree-of-freedom vibration-isolation system under different damping ratios

4 Conclusions

In this paper, for the topside module of the large floating structure FPSO, the overall vibration reduction technology of elastic connection with the hull is adopted. That is, elastomeric bearing pads are used to vertically support, horizontally limit,

and vertically anti-uplift the topside module. It can not only increase the buffering space of the topside module for the overall longitudinal bending of the hull to reduce the adverse effects of hull deformation on the topside module, but also reduce the vibration response of the topside module structure and isolate the transmission of vibration energy to the hull. Different from the vibration reduction or isolation of fixed marine structures or land buildings, the floating structures are always in the six-degree-of-freedom motion state. The motion response will directly affect the force and stress extremes of elastomeric bearing pads, which determines the applicability and feasibility of the vibration reduction technology in the operating sea area of the floating structures. In this paper, the vibration reduction effect of topsides and the vibration isolation performance of the elastomeric bearing pads system are verified via numerical simulation and theoretical analysis. The following conclusions are obtained after analysis:

1) Overall vibration reduction technology can achieve good vibration reduction and isolation effects. The overall vibration reduction setting of FPSO topside module can reduce the acceleration vibration response of the module structure, with a reduction efficiency of more than 30%, which can help to improve the working environment of operators. At the same time, the appropriate frequency ratio can be obtained through appropriate equipment selection of the excitation sources in the module, thus realizing a good vibration isolation effect of the hull.

2) Overall vibration reduction technology can reduce the maximum stress and fluctuation amplitude of the module structure, and thus improve the fatigue life of topsides. When the elastomeric supporting system achieves good vibration isolation effect, it can reduce the transmission of vibration energy from topsides to the hull, so as to reduce the maximum stress and fluctuation amplitude of the hull structure, and finally improve the fatigue life of the hull.

References

- [1] LI Y L, MU Q, ZU W, et al. Structural design of upper modular modification for FPSO [J]. *Ship & Boat*, 2015, 26(6): 45–49 (in Chinese).
- [2] KREKEL M H, KAMINSKI M L. FPSOs: design considerations for the structural Interface hull and topsides [C]//Offshore Technology Conference. Houston, Texas, USA: OTC, 2002: 6–9.
- [3] WEI Q. Research on integrated design of FPSO hull and upper module [D]. Zhenjiang: Jiangsu University of Science and Technology, 2021 (in Chinese).
- [4] MACHADO C L, SANTOS M A. Structural optimization on topside supports for ship-shaped hulls [C]//ASME2002 21st International Conference on Offshore Mechanics and Arctic Engineering. Oslo, Norway: ASME, 2002:23–28.
- [5] HENRIKSEN L O, BOYDEN D W, WANG X Z, et al. Structural design and analysis of FPSO topside module supports [C]//SNAME Maritime Convention. Houston, Texas, USA: SNAME, 2008: 17–18.
- [6] PAIK J K, THAYAMBALLI A K. *Topsides, mooring, and export facilities design* [M]. Cambridge: Cambridge University Press, 2007: 318–355.
- [7] MESPAQUE W, FRAINER V J, DE FREITAS TEIXEIRA P R. Analysis of hull–topside interaction by experimental approach on floating production unit P-53 [J]. *Applied Ocean Research*, 2012, 37: 133–144.
- [8] TANG Z F, WEN Z F, WANG S, et al. Discussion of the connection type between topside modules and hull of Cylinder FPSO [J]. *Petro&Chemical Equipment*, 2021, 24(10): 24–26 (in Chinese).
- [9] GAO Y. Research on fatigue characteristics and anti-fatigue design of FPSO topside module [D]. Tianjin: Tianjin University, 2018 (in Chinese).
- [10] ZHAO G X, LIU X M. The analysis of module stool of FPSO under severe sea state [J]. *Shanghai Shipbuilding*, 2004(1): 43–47 (in Chinese).
- [11] LI Q, CHEN Y, HUANG Z Q, et al. Dynamic mechanical analysis and experimental study of FPSO module stool in extreme sea conditions [J]. *Chinese Journal of Engineering Design*, 2020, 27(6): 698–706 (in Chinese).
- [12] LIAO H Q. Structural design for FPSO topside module [J]. *Shipbuilding of China*, 2008, 49(Supp 2): 232–238 (in Chinese).
- [13] CHI S Y, ZHAO G X. FPSO module stool structural forms and design principles [J]. *Naval Architecture and Ocean Engineering*, 2014(4): 24–27 (in Chinese).
- [14] ZHANG M, CHENG Y X. Investigation of FPSO module structure design [J]. *Ship Standardization Engineer*, 2018,51(1): 35–38, 59 (in Chinese).
- [15] LENG S D, YIN Y, YANG Q, et al. FPSO module stool design and strength assessment [J]. *Ship&Ocean Engineering*, 2017, 46(Supp 2): 227–229 (in Chinese).
- [16] LIU C H. Research of the installation technology for the topside modules of a 300 000 t FPSO [J]. *Petro&Chemical Equipment*, 2018, 21(12): 36–38 (in Chinese).
- [17] DU Z R. The application of spherical bearing to the assembling of a deep water FPSO [J]. *Shandong Chemical Industry*, 2019, 48(6): 159–162 (in Chinese).
- [18] SHANG J F, YIN B R, DU Z R, et al. The application of spherical bearing to the construction of FPSO [J]. *Shandong Chemical Industry*, 2021, 50(19): 190–191, 193 (in Chinese).

- [19] LIU C H, SHI L, XUE Y H, et al. Analysis of precise positioning method for large FPSO module installation [J]. *Naval Architecture and Ocean Engineering*, 2019, 35(2): 59–61 (in Chinese).
- [20] LIU C, HUANG S T. Flexible fastening design and application of FPSO modules [J]. *Ocean Engineering Equipment and Technology*, 2019, 6(Supp 1): 364–371 (in Chinese).
- [21] XU T T. Structural analysis of hull stool of pipe rack on FPSO [J]. *Petrochemical Design*, 2021, 38(2): 62–68 (in Chinese).
- [22] XU T T. Structural analysis of FPSO electrical house module and foundation against blast [J]. *Petroleum Engineering Construction*, 2020, 46(5): 76–82 (in Chinese).
- [23] XU T T. Design analysis on the elastomeric bearing and hull stool of super large FPSO topside module [J]. *China Offshore Oil and Gas*, 2019, 31(1): 161–168 (in Chinese).
- [24] European Committee For Standardization. Structural bearings-Part 3: elastomeric bearings: BS EN 1337-3: 2005 [S]. Brussels: European Committee for Standardization, 2005.
- [25] HUANG Y C, HE Y P, LIU Y D, et al. Study of the response characteristics of a spread moored FPSO in the bidirectional sea state [J]. *Ocean Engineering*, 2022, 264:112453.
- [26] Tsinghua University, China Academy of Building Research. Code for anti-collapse design of building structures: CECS 392-2014 [S]. Beijing: China Planning Press, 2014 (in Chinese).
- [27] DNVGL. Design of offshore steel structures, general LRFD method: DNVGL-OS-C101[S]. Oslo, Norway: DNVGL, 2015.
- [28] HAN D S, KIM M. The effect of reinforcing plate on the stiffness of elastomeric bearing for FPSO [J]. *Energies*, 2020, 13(24): 6640.
- [29] HAN D, CHE W. Comparison of the shear modulus of an offshore elastomeric bearing between numerical simulation and experiment [J]. *Applied Sciences*, 2021, 11(10): 4384.
- [30] ZHAO Y, WANG W, ZHOU Q, et al. Dynamic analysis of the reciprocating compressor package on the offshore platform [C]//IOP Conference Series: Materials Science and Engineering, 10th International Conference on Compressors and their Systems 11–13 September 2017. London, United Kingdom: IOP, 2017:11–13.
- [31] HUANG Z J, KIM H J. Physical modeling and simplification of FPSO topsides module in wind tunnel model tests [C]//ASME 2021 40th International Conference on Ocean, Offshore and Arctic Engineering. Virtual: ASME, 2021: 21–30.
- [32] Ministry of Housing and Urban-Rural Development of the People's Republic of China, General Administration of Quality Supervision, Inspection and Quarantine of the People's Republic of China. Code for seismic design of buildings: GB 50011–2010 [S]. Beijing: China Architecture & Building Press, 2010 (in Chinese).
- [33] European Committee for Standardization. Eurocode 8: Design of structures for earthquake resistance-Part 2: Bridges: BS EN 1998-2:2005 [S]. Brussels: European Committee for Standardization, 2005.
- [34] MAGHSOUDI-BARMI A, KHALOO A, MOEINI M E. Experimental investigation of unbonded ordinary steel reinforced elastomeric bearings as an isolation system in bridges [J]. *Structures*, 2021, 32: 604–616.
- [35] Bureau Veritas. Comfort and health on-board offshore Units: BV NR636 DT R00 E [S]. [S. l.]: Marine & Offshore Division, 2016.
- [36] JIN X D, XIA L J. Ship vibration[M]. Shanghai: Shanghai Jiao Tong University Press, 2011 (in Chinese).
- [37] JI M P. Study and optimization of the flexible isolation system [D]. Shantou: Shantou University, 2013 (in Chinese).

基于弹性连接的FPSO上部模块整体减振技术

黄雨促^{1,2,3}, 何炎平^{*1,2,3}, 仇明⁴, 刘亚东^{1,2,3}, 李铭志^{1,2,3}

1 上海交通大学 海洋工程全国重点实验室, 上海 200240

2 上海交通大学 船舶海洋与建筑工程学院, 上海 200240

3 上海交通大学 海洋装备研究院, 上海 200240

4 启东中远海运海洋工程有限公司, 江苏 启东 226259

摘要: [目的] 针对浮式生产储卸油装置(FPSO)作业时上部模块的振动响应, 为减少振动能量向船体的传递, 同时改进上部模块与船体之间的连接, 提出一种基于上部模块与船体弹性连接的整体减振技术。[方法] 首先, 利用弹性支座将上部模块与船体进行弹性连接, 根据FPSO在作业海域加速度响应预报的极值来确定弹性支座的设计载荷和内部结构; 然后, 采用有限元方法分析弹性支座的受力与变形特性, 并通过线性拟合获得弹性支座的等效刚度; 最后, 将弹性支座等效为线性弹簧, 分别通过数值模拟和理论分析来研究模块结构的振动响应和弹性支撑系统的动力传递特性。[结果] 结果表明: 应用该减振技术之后, 上部模块的减振效率高达30%以上, 同时还可使船体取得良好的隔振效果。[结论] 该研究成果可为海洋结构物上部模块的整体减振设计和应用提供参考。

关键词: 浮式生产储卸油装置; 上部模块; 弹性连接; 整体减振